BIOCHEMISTRY
including biophysical chemistry & molecular biology

Rapid Report

pubs.acs.org/biochemistry

Effect of Loop Sequence and Loop Length on the Intrinsic Fluorescence of G-Quadruplexes

Chun Kit Kwok, Madeline E. Sherlock, and Philip C. Bevilacqua*

Department of Chemistry, Center for RNA Molecular Biology, Pennsylvania State University, University Park, Pennsylvania 16802, United States

Supporting Information

ABSTRACT: Guanine quadruplex structures (GQSs) exhibit unique spectroscopic features, including an inverse melting profile at 295 nm, distinctive circular dichroism features, and intrinsic fluorescence. Herein, we investigate effects of loop sequence and loop length on the intrinsic fluorescence of 13 DNA GQSs. We report label-free fluorescence enhancements upon intramolecular GQS formation of up to 16-fold and a shift in the emission maximum to the visible portion of the spectrum. Effects can be understood in the context of available nuclear magnetic resonance GQS structures. The intrinsic fluorescence of GQSs may be useful for nucleic acid studies and for the development of label-free detection methods.

Guanine quadruplex structures (GQSs) have been of great interest for decades. They are found in DNA telomere repeats and the promoter region of certain proto-oncogenes, such as c-myc, c-kit, and bcl-2.[1−3] Guanine-rich sequences in DNA or RNA can potentially form a GQS if they contain the pattern $G_xL_aG_xL_bG_xL_cG_x$, where $x \geq 2$ and loops a, b, and c consist of at least one nucleotide. The four stretches of G's interact with one another to form two or more quartets that stack upon each other, with the backbone in a parallel or antiparallel geometry. Formation of the GQS requires dehydrated K^+ or Na^+ to be present between or within the stacked quartet planes, which stabilizes charge accumulation from having four adjacent strands.[4] Detailed ion binding studies have been performed on diverse GQS contexts under various ionic strength conditions, and the general consensus is that they prefer K^+ over other ions.[5−7]

The unique structure and folding of GQSs lead to distinctive spectroscopic features as compared to those of other nucleic acid motifs. For example, the GQS has a characteristic "inverse" or hypochromic melting profile when monitored at 295 nm, in which absorbance decreases as the structure unfolds.[8] The GQS also has characteristic patterns in circular dichroism (CD) experiments: for a parallel topology, there is a positive peak near 260−265 nm with a minimum near 245 nm, whereas for an antiparallel topology, there are positive peaks at 245 and 295 nm with a minimum near 260−265 nm.[9] The intrinsic fluorescence of DNA GQSs was reported recently[10] and is also likely due to the extended conjugation of the four-base quartet. Fluorescence studies of DNA GQSs to date have been conducted primarily on the telomeric GQS sequence.[11−13] Our lab recently reported that RNA GQSs exhibit intrinsic fluorescence as well. We showed that the folding cooperativity of a GQS, which can be tuned by adjusting the loop sequence or number of guanines in each stretch,[14,15] can be assessed by monitoring GQS fluorescence as a function of K^+ concentration.[15]

There is, however, little knowledge of what parameters influence the intrinsic fluorescence of GQSs. It seemed likely that loop sequence and length would play important roles in fluorescence given the key roles that these structural features play in GQS folding and stability.[6,16,17] In this study, we conduct fluorescence measurements to investigate the effect of loop sequence and length on the intrinsic fluorescence of dG_2 and dG_3 GQSs upon K^+ titration. We then characterize the molecularity and folding cooperativity of a highly fluorescent sequence, dG_3T, compare it to its A-loop counterpart and available structures, and discuss advantages and potential applications of intrinsic GQS fluorescence.

To investigate the effects of loop sequence and length on GQS fluorescence, we designed 13 DNA GQSs with various single-base loops (A, C, or T),[a] loop lengths (1−3 nucleotides), and G-stretch lengths.[2,3] To simplify the study, the loops within each GQS were chosen to comprise a single base but be of variable length, following the pattern "dG_xL_y", where x and y represent the number of quartets and loop nucleotides, respectively. The DNA GQS motifs used in this study and their abbreviations are listed in Table 1.[b]

The GQS topology was determined by monitoring the ellipticity at 5 μM DNA and 10 mM lithium cacodylate (pH 7.0) at 1 M K^+. The CD and fluorescence spectra for all 13 sequences are provided in Figures S1−S13 of the Supporting Information, and the GQS topologies are summarized in Table 1. The CD results reveal that GQSs with loops with one nucleotide (i.e., dG_2L and dG_3L) have parallel topologies as expected.[6,18] GQSs with longer loops were found by comparison to CD to be parallel, antiparallel, or a combination of the two topologies (Table 1).

To compare fluorescence intensities in unfolded, physiological K^+, and saturated K^+ states, we collected fluorescence data on each sequence at 0, 100, and 1000 mM K^+ (Figure 1A). We found that the wavelength of maximal emission varies by ∼80 nm among the GQSs, ranging from 340 to 420 nm (Table 1 and Figures S1−13 of the Supporting Information). In general, dG_3L_y GQSs are more fluorescent than their dG_2L_y counterpart (Figure

Received: February 3, 2013
Revised: March 24, 2013
Published: April 26, 2013

   dx.doi.org/10.1021/bi400139e | *Biochemistry* 2013, 52, 3019−3021

Table 1. DNA GQS Sequences, Topologies, and Emission Wavelength Maxima

dG_xL_y	sequence	topology[a]	λ_{em} (nm)[b]
dG_2A	GGAGGAGGAGG	parallel	400
dG_2A_2	GGAAGGAAGGAAGG	parallel	410
dG_2A_3	GGAAAGGAAAGGAAAGG	parallel	420
dG_2T	GGTGGTGGTGG	parallel	385
dG_2T_2	GGTTGGTTGGTTGG	antiparallel	385
dG_2T_3	GGTTTGGTTTGGTTTGG	antiparallel	NA[c]
dG_3A	GGGAGGGAGGGAGGG	parallel	385
dG_3A_2	GGGAAGGGAAGGGAAGGG	antiparallel	340, 420
dG_3A_3	GGGAAAGGGAAAGGGAAAGGG	antiparallel	390
dG_3T	GGGTGGGTGGGTGGG	parallel	390
dG_3T_2	GGGTTGGGTTGGGTTGGG	parallel	380
dG_3T_3	GGGTTTGGGTTTGGGTTTGGG	mixed[d]	340
dG_3C	GGGCGGGCGGGCGGG	parallel	390

[a]Topology judged by CD spectroscopy at 1 M K^+. [b]Values determined by peak maxima in the emission spectrum at 1 M K^+ with excitation at 260 nm. [c]The fluorescence was weak, and the peak wavelength was not available (NA). [d]Assigned as mixed because CD has positive ellipticity at both 260 and 295 nm.

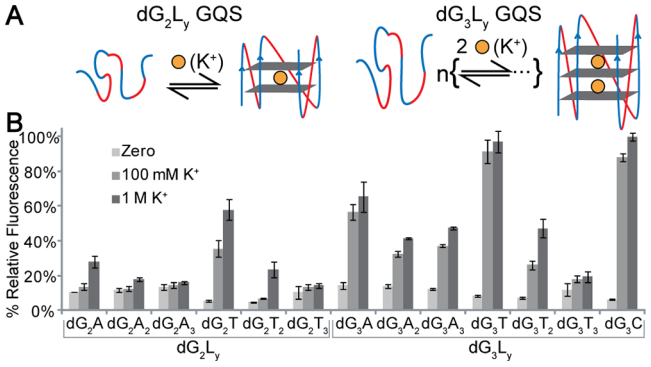

Figure 1. Experimental design and fluorescence titration results. (A) GQS folding model for the dG_2L_y GQS (left) and dG_3L_y GQS (right). The guanine stretches (G_x) are colored blue and the loops (L_y) red. dG_2L_y and dG_3L_y GQSs with parallel topologies are depicted in panel A, although antiparallel quartets are found (Table 1). (B) Relative fluorescence intensity of an individual GQS upon K^+ titration. The fluoresence intensity for each GQS was obtained at the λ_{em} shown in Table 1; for dG_2T_3, we chose the fluorescence intensity at 340 nm (see Figure S6B of the Supporting Information). Experiments were performed at 5 μM, with identical instrument settings, and the highest fluorescence intensity was normalized as 100%.

1B). In addition, GQSs with loops with one nucleotide have significantly higher fluorescence emission under saturating K^+ conditions than loops with two or three nucleotides. Indeed, for T loops, fluorescence decreases markedly with increasing loop size, for both dG_2 and dG_3 sequences, to the point where there is almost no fluorescence for the T_3 loop sequences (Figure S14-S15 of the Supporting Information). Of the dG_2L_y GQSs tested, dG_2T is the most fluorescent, being ~2−6 times more fluorescent than the other GQS-forming dG_2L_y sequences. Among all DNA GQSs tested, dG_3T and dG_3C achieve the highest overall fluorescence in 1 M K^+, as well as the largest enhancement in fluorescence, ~12- and ~16-fold, respectively, upon GQS formation (Figure 1B).

We selected dG_3T for further spectroscopic and thermodynamic evaluation because nuclear magnetic resonance (NMR) structural information is available for it.[19] Full K^+ titrations were performed, which led to a $K^+_{1/2}$ value of 1.2 ± 0.4 mM and a Hill coefficient (n) of 0.57 ± 0.02 (Figure 2A,B). The low value of n

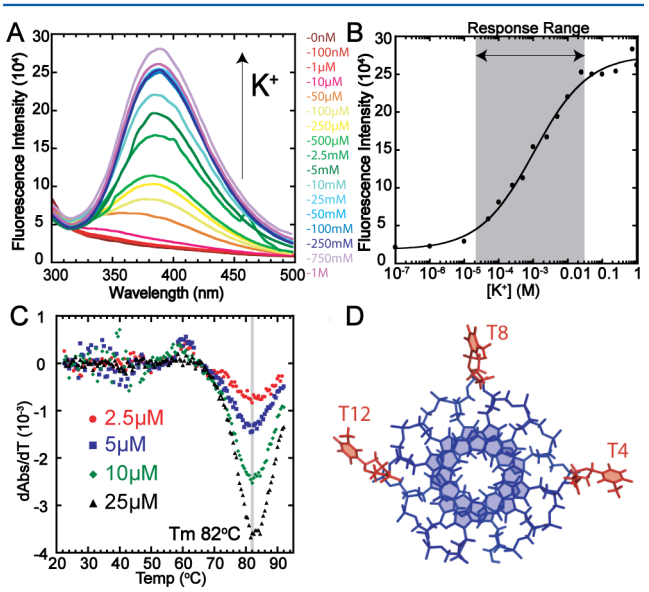

Figure 2. Characterization of dG_3T. (A and B) Emission spectra and K^+ titration plot monitored at 390 nm for dG_3T. The $K^+_{1/2}$ and the Hill coefficient (n) are 1.2 ± 0.4 mM and 0.57 ± 0.02 using eq S1. The average was obtained from three experiments, and the error is the standard deviation. The response range (10−90% signal) of dG_3T is shaded gray. (C) UV melting of dG_3T monitored at 295 nm at various concentrations. The vertical bar shows the position of the T_m. (D) NMR structure of $d(GGGT)_4$ (PDB entry 2LE6).[19] The 3′-terminal T (T16) is not shown. Loops and G-quartets are colored red and blue, respectively.

indicates that GQS folding is anticooperative, which is also reflected in the wide, ~1000-fold analyte response range. Such anticooperativity is consistent with our recent GQS folding studies with long RNA GQSs.[14,15] In addition, UV melting was monitored at 295 nm at dG_3T concentrations ranging from 2.5 to 25 μM, and the melting temperature (T_m) was found to be independent of concentration (Figure 2C), indicating that the fluorescence signal observed at 5 μM dG_3T K^+ titration is due to intramolecular GQS folding.

Our results indicate that the increase in fluorescence observed upon K^+ titration is due to formation of GQSs, as GQS-specific signals were observed in the CD under these conditions (Figure S1−13 of the Supporting Information). Likewise, non-GQS-forming sequences did not exhibit an increase in fluorescence upon K^+ titration.[10,b] We also tested different anions (fluoride and acetate) and found that fluorescence intensity changes were similar to those with chloride (data not shown), suggesting absence of anion induced quenching. Comparison of fluorescence intensity among GQS candidates at 1 M K^+ is justified, as plateaus were observed at higher K^+ concentrations, indicating that the GQS is in its fully folded states (Figure S14 of the Supporting Information). The origin of GQS intrinsic fluorescence is proposed to be contributed by a ^{1}G*G excimer.[10] It is likely that the loop sequence and length alter the GQS, thereby affecting the excited states and energy transfer properties of GQSs.

It is of interest to correlate the spectroscopic observations herein with GQSs. An NMR structure is available for 5′-$d(GGGT)_4$,[19] which has the same CD profile and T_m within 2 °C of that of dG_3T.[20] In the structure, the T-loops are extruded and

dx.doi.org/10.1021/bi400139e | Biochemistry 2013, 52, 3019−3021

do not interact with the G-quartets (Figure 2D). The flipped-out nature of the loop bases is likely responsible for the stronger fluorescence of this GQS, as T's are known to quench fluorescence.[21] Because dG_3C had a relative fluorescence intensity and an emission wavelength maximum similar to those of dG_3T, and the same topology as dG_3T (both parallel) (Table 1), it is likely that the one-pyrimidine loops of dG_3C and dG_3T are extruded. The strong decrease in fluorescence with T-loop length (Figure S15 of the Supporting Information) likely arises because lengthening the extruded loops leads to enhanced collisional quenching by the thymines.

As compared to dG_3C and dG_3T, dG_3A has significantly weaker fluorescence. Moreover, among the dG_2L sequences, dG_2A has significantly lower fluorescence than dG_2T. Interestingly, an NMR structure of 5′-$d(GGA)_4$, similar in sequence to dG_2A, reveals that the A's interact with the G-quartet to form a heptad structure (Figure S16 of the Supporting Information).[22] It is likely that such direct GQS interactions quench fluorescence in dG_2A and dG_3A.

The dependence of the maximal emission wavelength on loop sequence can also be correlated with GQSs. In particular, dG_2A_{1-3} emits at the longest wavelengths, with emission maxima of 400−420 nm, whereas dG_2T_{1-2} has emission maxima of ∼385 nm (Table 1 and Figure S15 of the Supporting Information). Apparently, the heptads present in the A-loop GQS extend the conjugation of the G-quartet leading to the shift in fluorescence into the visible light portion of the spectrum. Notably, two peaks were observed in the fluorescence emission of dG_3A_2, one at 340 nm and the other at 420 nm (Figure S8 of the Supporting Information), which suggests that the quartets in dG_3A_2 may experience different environments, one with a heptad and one without.

The strong fluorescence enhancement and wide dynamic range of K^+ detection of dG_3T upon GQS folding demonstrate its merit for sensor development and broad response range K^+ detection. The intrinsic fluorescence of GQSs can be used in fluorescence melting, kinetics, or quadruplex primer amplification (QPA) readouts[20] without the incorporation of unnatural bases such as 2-aminopurine (2-AP), which have been found to affect the T_m of the dG_3T GQS[23] and to interfere with certain biological studies. Moreover, the intrinsic fluorescence of dG_3T could be utilized as a readout to replace a GQS ligand binding reporter such as ZnPPIX in the G-quadruplex integrated hybridization chain reaction (GQ-HCR).[24]

In summary, we have investigated the intrinsic fluorescence of DNA GQSs with various loops sequences and lengths. We observe a wide dynamic range of emission intensity and maxima, and these can be understood in light of available NMR structures. The label-free fluorescence of the GQS motif described provides a tool for nucleic acid studies and sensor development where fluorescence output is desired.

■ ASSOCIATED CONTENT

Supporting Information

Materials and methods and Figures S1−S16. This material is available free of charge via the Internet at http://pubs.acs.org.

■ AUTHOR INFORMATION

Corresponding Author

*E-mail: pcb5@psu.edu. Phone: (814) 863-3812.

Author Contributions

C.K.K. and M.E.S. are joint first authors.

Funding

This study was supported by Human Frontier Science Program (HFSP) Grant RGP0002/2009-C to P.C.B. and Penn State Summer Discovery Grant to M.E.S.

Notes

The authors declare no competing financial interest.

■ ACKNOWLEDGMENTS

We thank Prof. Christine Keating for use of the fluorimeter.

■ ADDITIONAL NOTES

[a]We did not study loops of G's as these would lead to heterogeneous mixtures of states.

[b]According to CD, dG_2C, dG_3C_2, and dG_3C_3 were not found to form GQSs presumably because of competitive Watson−Crick structures (data not shown). It appears that for dG_xC_y to form a GQS, x and y should be no less than two.

■ REFERENCES

(1) Balasubramanian, S., and Neidle, S. (2009) *Curr. Opin. Chem. Biol. 13*, 345−353.

(2) Sannohe, Y., and Sugiyama, H. (2010) *Curr. Protoc. Nucleic Acid Chem.*, Chapter 17:Unit 17.2, pp 1−17, Wiley, New York.

(3) Biffi, G., Tannahill, D., McCafferty, J., and Balasubramanian, S. (2013) *Nat. Chem. 5*, 182−186.

(4) Halder, K., and Hartig, J. S. (2011) *Met. Ions Life Sci. 9*, 125−139.

(5) Hud, N. V., Smith, F. W., Anet, F. A. L., and Feigon, J. (1996) *Biochemistry 35*, 15383−15390.

(6) Bugaut, A., and Balasubramanian, S. (2008) *Biochemistry 47*, 689−697.

(7) Zhang, A. Y. Q., Bugaut, A., and Balasubramanian, S. (2011) *Biochemistry 50*, 7251−7258.

(8) Mergny, J.-L., Phan, A.-T., and Lacroix, L. (1998) *FEBS Lett. 435*, 74−78.

(9) Vorlíčková, M., Kejnovská, I., Sagi, J., Renčiuk, D., Bednářová, K., Motlová, J., and Kypr, J. (2012) *Methods 57*, 64−75.

(10) Mendez, M. A., and Szalai, V. A. (2009) *Biopolymers 91*, 841−850.

(11) Miannay, F.-A., Banyasz, A., Gustavsson, T., and Markovitsi, D. (2009) *J. Phys. Chem. C 113*, 11760−11765.

(12) Dao, N. T., Haselsberger, R., Michel-Beyerle, M.-E., and Phan, A. T. (2011) *FEBS Lett. 585*, 3969−3977.

(13) Hua, Y., Changenet-Barret, P., Improta, R., Vayá, I., Gustavsson, T., Kotlyar, A. B., Zikich, D., Šket, P., Plavec, J., and Markovitsi, D. (2012) *J. Phys. Chem. C 116*, 14682−14689.

(14) Mullen, M. A., Assmann, S. M., and Bevilacqua, P. C. (2012) *J. Am. Chem. Soc. 134*, 812−815.

(15) Kwok, C. K., Sherlock, M. E., and Bevilacqua, P. C. (2013) *Angew. Chem., Int. Ed. 52*, 683−686.

(16) Guédin, A., De Cian, A., Gros, J., Lacroix, L., and Mergny, J.-L. (2008) *Biochimie 90*, 686−696.

(17) Guédin, A., Gros, J., Alberti, P., and Mergny, J.-L. (2010) *Nucleic Acids Res. 38*, 7858−7868.

(18) Hazel, P., Huppert, J., Balasubramanian, S., and Neidle, S. (2004) *J. Am. Chem. Soc. 126*, 16405−16415.

(19) Do, N. Q., Lim, K. W., Teo, M. H., Heddi, B., and Phan, A. T. (2011) *Nucleic Acids Res. 39*, 9448−9457.

(20) Kankia, B. I. (2011) *Anal. Biochem. 409*, 59−65.

(21) Kierzek, R., Li, Y., Turner, D. H., and Bevilacqua, P. C. (1993) *J. Am. Chem. Soc. 115*, 4985−4992.

(22) Matsugami, A., Ouhashi, K., Kanagawa, M., Liu, H., Kanagawa, S., Uesugi, S., and Katahira, M. (2001) *J. Mol. Biol. 313*, 255−269.

(23) Johnson, J., Okyere, R., Joseph, A., Musier-Forsyth, K., and Kankia, B. (2013) *Nucleic Acids Res. 41*, 220−228.

(24) Dong, J., Cui, X., Deng, Y., and Tang, Z. (2012) *Biosens. Bioelectron. 38*, 258−263.